Journal of Colloid and Interface Science 570 (2020) 173–181

Contents lists available at ScienceDirect

Journal of Colloid and Interface Science

journal homepage: www.elsevier.com/locate/jcis

Unraveling the mystery of ultrafine bubbles: Establishment of thermodynamic equilibrium for sub-micron bubbles and its implications

Euna Kim [a,b], Jong Kwon Choe [a], Byung Hyo Kim [c,d], Joodeok Kim [c,d], Jungwon Park [c,d], Yongju Choi [a,*]

[a] Department of Civil and Environmental Engineering, Seoul National University, Seoul 08826, Republic of Korea
[b] Department of Civil and Environmental Engineering, University of Southern California, Los Angeles, CA 90089, United States[1]
[c] Center for Nanoparticle Research, Institute for Basic Science, Seoul 08826, Republic of Korea
[d] School of Chemical and Biological Engineering, and Institute of Chemical Process, Seoul National University, Seoul 08826, Republic of Korea

GRAPHICAL ABSTRACT

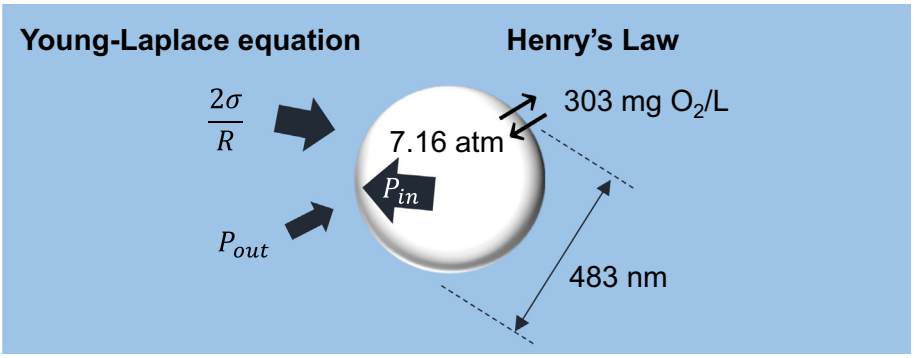

ARTICLE INFO

Article history:
Received 12 November 2019
Revised 24 February 2020
Accepted 25 February 2020
Available online 26 February 2020

Keywords:
Ultrafine bubble
Supersaturation
Laplace pressure
Bubble size
Henry's law

ABSTRACT

Hypothesis: We test the validity of the Young-Laplace equation and Henry's law for sub-micron bubble suspensions, which has long been a questionable issue. Application of the two theories allows characterization of bubble diameter and gas molecule partitioning between gaseous and dissolved phases using two easily measurable variables: total gas content (C_T) and bubble volume concentration (*BVC*).
Experiments: We measure C_T and *BVC* for sub-micron bubble suspensions generated from three pure gases, which allows calculation of bubble diameter for each suspension using the Young-Laplace equation and Henry's law. Uncertainties involved in the experimental measurements are assessed. Bubble size for each suspension is also directly measured using a dynamic light scattering (DLS) technique for comparison.
Findings: Applying the two theories we calculate that the bubble diameters are in the range of 304–518 nm, which correspond very well with the DLS-measured diameters. Sensitivity analyses demonstrate that the correspondence of the calculated and DLS-measured bubble diameters should take place only if the two theories are valid. The gas molecule partitioning analysis shows that >96% of gas molecules in the suspension exist as dissolved phase, which suggests the significance of the dissolved phase for applications of the bubble suspensions.

1. Introduction

Ultrafine bubbles, which refers to gas bubbles with a dimension of a micron or smaller [1], are currently drawing substantial atten-

* Corresponding author at: 35-307, Seoul National University, 1 Gwanak-ro, Gwanak-gu, Seoul 08826, Republic of Korea.
E-mail address: ychoi81@snu.ac.kr (Y. Choi).
[1] Present address.

https://doi.org/10.1016/j.jcis.2020.02.101
0021-9797/

tion among scientists and engineers with an expectation that they would lead innovation in various fields. With a much smaller size compared to conventional macrobubbles (a few millimeters in size) and microbubbles (a few micrometers to 50 μm in size), ultrafine bubbles exhibit unique properties such as high stability in aqueous solutions (residence time reported up to several tens or hundreds of days) [2], rapid mass transfer at the bubble-water interface [3,4], high dissolved gas concentration in the water containing the bubbles [5], and high negative pressure at the surface [6,7]. In the field of water treatment, these unique properties of ultrafine bubbles have been exploited to achieve enhanced ozone supply for chemical oxidation of water and groundwater contaminants [8,9], improved flotation efficiency for solids separation, and better fouling control in membrane separation processes [10]. Application of oxygen/air ultrafine bubbles in biological water and wastewater treatment and groundwater bioremediation has been suggested as a means to substantially enhance the aeration efficiency, which, in turn, may improve the performance of the treatment [11]. In agricultural science, enhanced aeration by oxygen ultrafine bubbles has been successfully demonstrated to promote plant and animal growth [12,13]. Oxygen ultrafine bubbles have shown a great potential in medical treatments by serving as an oxygen carrier to supply oxygen to injured tissues or for inactivating anaerobic bacteria on infected skin [14–16].

Despite the rapid growth of the literature demonstrating the potential applicability of ultrafine bubbles, the physicochemical properties of ultrafine bubbles, particularly those related to the stability of the bubbles, remain to be poorly understood [17]. The resistance to buoyancy and bubble coalescence is relatively well explained by the low rising velocity of ultrafine bubbles that allows Brownian motion to dominate the bubble movement and the electrostatic repulsion between the bubbles, respectively [2,11,18,19]. On the other hand, it is questionable how thermodynamic equilibrium is established (or if it is really established) at the gas-water interface such that the bubble retains its size without significant growth or dissolution for a sufficiently long time as observed in many studies [3,18,20]. As the classical theories that have been believed to be universally applicable to gas-water interface indicate that it becomes less and less feasible to obtain a thermodynamic equilibrium as bubble size gets smaller, many scientists regard the observed stability of ultrafine bubbles as a mystery [17,21].

One may expect two classical theories to be applicable at the gas-water interface of the bubbles in water. The first one is the Young-Laplace equation, which can be written for a spherical bubble as [17,21]:

$$\Delta p = p_{in} - p_{out} = 2\gamma/r \tag{1}$$

where p_{in} (Pa) is the inner pressure the bubble (gaseous phase); p_{out} (Pa) is the outer pressure of the bubble (aqueous phase); γ (N m^{-1}) is the surface tension of water; and r (m) is the bubble radius. This equation tells that, given that the surface tension remains constant, the inner pressure of the bubble gets larger as the bubble size gets smaller. For an aqueous suspension with 1 atm (=1.013 × 10^5 Pa) in pressure and 20 °C in temperature, the Young-Laplace equation returns an inner pressure of 29.7 atm for a bubble with 100 nm in diameter and 288 atm for 10 nm in diameter. The other theory applicable to the gas-water interface in thermodynamic equilibrium is Henry's law, which can be represented for a bubble by [22]:

$$p_{in} = H_{pc} \cdot C_{aq,eq} \tag{2}$$

where H_{pc} (N m mol^{-1}) is the Henry's law constant and $C_{aq,eq}$ (mol m^{-3}) is the dissolved concentration of the gas molecule in the surrounding water at equilibrium. For a bubble made of pure oxygen in an aqueous suspension at 1 atm, 20 °C to satisfy Eqs. (1) and (2), $C_{aq,eq}$ should be 39.28 mol m^{-3} (or 1257 mg L^{-1}) and 380.95 mol m^{-3} (or 12.2 g L^{-1}) if the bubble diameters are 100 nm and 10 nm, respectively.

The calculation above implies that for sufficiently small bubbles, the two classical theories may fail to explain the stability of the bubbles, or otherwise, the constants in Eq. (1) and/or Eq. (2) (surface tension of water and the Henry's law constant, respectively) should be substantially modified. In other words, there should be a bubble size range in which the bubble characteristics are dependent on unique mechanisms applicable at very small dimensions rather than those that governs the gas-water interface at a macroscopic scale. This is not surprising if an analogy is drawn to nanoparticles, which have been found to exhibit significantly different physicochemical properties compared to macroscale particles with the same composition [23–25]. Here, a follow-up statement that can be made is that down to a certain size range, the physicochemical characteristics of bubbles observable at a macroscopic scale will remain to be valid.

In this study, we hypothesize that for ultrafine bubbles with a size of a few hundred nanometers (i.e., sub-micron-sized bubbles), the two classical theories (i.e., the Young-Laplace equation and Henry's law) can still reasonably be applicable for the gas-liquid interface. Because most of the bulk ultrafine bubbles studied in the literature or employed in practical applications are in this size range, the validity of this assumption has many implications. Given that the two theories are applicable, it is possible to estimate the bubble size and counts, and to understand how much gas molecules the bubble suspension carries in aqueous and gaseous phases, respectively (i.e., the phase partitioning of gas molecules), using a very simple laboratory procedure that can be performed in any laboratory settings.

In the following section, we illustrate how the properties of an ultrafine bubble suspension listed above (i.e., bubble size, bubble counts, and aqueous/gaseous phase partitioning of gas molecules) can be estimated using Eqs. (1) and (2) with measurement of two macroscopic properties of the suspension: total gas content and bubble volume concentration (*BVC*). Using the total gas content and *BVC* values determined for ultrafine bubble suspensions generated in the laboratory, the suspension properties are estimated. The calculated value of a key bubble suspension property, i.e., the bubble size, is compared with the results from an instrumental measurement. This study design allows testing the hypothesis that the two classical theories are applicable to sub-micron-sized bubbles and providing a simple experimental procedure to determine ultrafine bubble suspension properties at the same time.

2. Theoretical analysis

2.1. Phase partitioning of gas molecules in an ultrafine bubble suspension

It is challenging to determine how much fraction of gas molecules exists in either bubbles (gaseous phase) or dissolved (aqueous) phase in an ultrafine bubble suspension. Because an ultrafine bubble suspension behaves as a system where bubbles and the aqueous phase continuously interact with each other to exhibit its overall characteristics, any attempt to separate the two phases may result in disturbance in such interactions, leading to significant errors in the determination of the phase partitioning of the gas molecules. It was suggested that signals of dissolved oxygen (DO) meters may represent or infer the concentration of oxygen that is actually dissolved in an ultrafine bubble suspension [17]. However, for oxygen ultrafine bubble suspensions generated in the current study, the signal of the DO meter (ProODO, YSI Inc., USA; measures DO by an optical method) exceeded the upper measurement limit of 90 mg L^{-1}. This suggested that the DO concentration of the oxygen ultrafine bubble suspensions generated in this

study was remarkably higher than the typical measurement range and that an accurate determination of DO concentration was challenging via direct measurement using any DO meters. To address this challenge, based on classical theories that do or are assumed to apply to an ultrafine bubble suspension, we developed a method to determine the phase partitioning of gas molecules as described below.

By applying the ideal gas law and by defining the bubble volume concentration (*BVC*) as the total volume occupied by bubbles in a unit volume of a bubble suspension, the inner pressure of an ultrafine bubble is written as

$$p_{in} = (n_g \cdot R \cdot T)/V^b = (C_g \cdot V^s \cdot R \cdot T)/V^b = (C_g \cdot R \cdot T)/BVC \quad (3)$$

where n_g (mol) is the number of moles of gas molecules in ultrafine bubbles; R (=8.314 N m K^{-1} mol^{-1}) is the ideal gas constant; T (K) is the temperature; V^b (m^3) is the volume occupied by ultrafine bubbles; V^s (m^3) is the bubble suspension volume; C_g (mol m^{-3}) is the concentration of the gas molecules that exist in gaseous phase (i.e., in bubbles) on suspension volume basis; and $BVC = V^b/V^s$ (unitless) is the bubble volume concentration. The ideal gas law is valid within 5% error unless the gas pressure is extremely large (e.g., more than 100 atm for oxygen) [26]. Applying Henry's law (Eq. (2)) to an ultrafine bubble suspension, the inner pressure of ultrafine bubbles, p_{in}, can also be written as follows:

$$p_{in} = H_{pc} \cdot C_{aq} = H_{pc} \cdot (C_T - C_g) \quad (4)$$

where C_{aq} (mol m^{-3}) is the concentration of the gas molecules that exist in aqueous phase on suspension volume basis; and C_T (mol m^{-3}) is the total gas content (i.e., the concentration of the gas molecules that exist in any phase on suspension volume basis). Combining Eqs. (3) and (4), the following expression is obtained for the gas molecule concentration in bubbles of a suspension.

$$C_g = (H_{pc} \cdot C_T)/\{H_{pc} + (R \cdot T)/BVC\} \quad (5)$$

Therefore, if Henry's law holds for an ultrafine bubble suspension generated using a certain species of pure gas at a given temperature, C_g can be calculated using experimentally determined values of C_T and *BVC*. Experimental approaches to measure the two variables in an ultrafine bubble suspension are detailed in the Materials and methods Section. The fraction of gas molecules in gaseous and aqueous phases (R_g and R_{aq}, respectively) in a bubble suspension is given as follows.

$$R_g = C_g/C_T = H_{pc}/\{H_{pc} + (R \cdot T)/BVC\} \quad (6)$$

$$R_{aq} = C_{aq}/C_T = (R \cdot T)/\{H_{pc} \cdot BVC + R \cdot T\} \quad (7)$$

2.2. Bubble diameter and population

Combination of Eqs. (1), (3), and (5) gives

$$(H_{pc} \cdot C_T \cdot R \cdot T)/(H_{pc} \cdot BVC + R \cdot T) - p_{out} = 4\gamma/D \quad (8)$$

where D (m) is the bubble diameter. Rearrangement of Eq. (8) enables the calculation of the bubble diameter using given and experimentally measured values.

$$D = 4\gamma/\{(H_{pc} \cdot C_T \cdot R \cdot T)/(H_{pc} \cdot BVC + R \cdot T) - p_{out}\} \quad (9)$$

In the current study as well as for most of experimental systems and practical applications of ultrafine bubble suspensions, p_{out} can safely be assumed to be equivalent to the atmospheric pressure. The bubble population, n (counts m^{-3}), is given as

$$n = 6BVC/\pi D^3 \quad (10)$$

where π is the circular constant.

3. Materials and methods

3.1. Ultrafine bubble generation

An ultrafine bubble generator used in this study was a splitter-type device (see Fig. 1). When water containing macro-sized bubbles was injected to the splitter, which was essentially a coiled polyvinyl chloride (PVC) tubing 4 mm in inner diameter and 10 m in length, the high shear stress generated by the passage of the bubble suspension at high velocity broke up the macrobubbles, releasing a water suspension containing ultrafine bubbles at the outlet.

Both the water inlet and the bubble suspension outlet of the ultrafine bubble generator were connected to a reservoir to form a circulation system. The reservoir was filled with 500 mL of deionized (DI) water (except for the *BVC* measurement experiment which used a 5-L reservoir) prior to the generator operation. The gas inlet was connected to a tank supplying a pure gas of oxygen, nitrogen, or helium (>99.95% purity for each). The generator was operated at a gas flowrate of 30 mL min^{-1} using a gas regulator and a gas-water mixture flowrate of 300 mL min^{-1} using a peristaltic pump. To ensure the system to reach a steady state, the generator was run for at least 3.5 × the hydraulic retention time (HRT) of the reservoir. Afterwards, the bubble suspension prepared in the reservoir was used for measurement. The atmospheric and reservoir temperature was maintained at 25 ± 0.5 °C during the bubble generation as well as the measurements.

3.2. Bubble volume concentration (BVC) measurement

Bubble volume concentration (*BVC*) represents the total volume occupied by bubbles in a unit volume of a bubble suspension. This parameter was experimentally determined by measuring the volume change after completely removing bubbles in a suspension. Because the fraction of volume occupied by ultrafine bubbles was infinitesimal, a relatively large volume (5 L) of a suspension was generated in a volumetric flask-type reservoir which was designed to track volume change down to 0.01-mL resolution. Details on the reservoir design and the measurement procedure are provided in the Supplementary Materials. To remove bubbles from a bubble suspension, a 30-min gas purging was applied. The gas used for purging was pure nitrogen for oxygen and helium ultrafine bubbles and pure helium for nitrogen ultrafine bubbles. This procedure effectively destabilized an ultrafine bubble suspension, resulting in bubble coalescence and subsequent bubble rise to the surface.

3.3. Total gas content measurement

The total content of a given species of gas molecules in an ultrafine bubble suspension was determined using a head space gas pressure measurement technique developed in this study as follows. A 160-mL serum bottle (Wheaton, USA) was filled with approximately 60 mL of an ultrafine bubble suspension generated using a pure gas (i.e. oxygen, nitrogen, or helium), and the headspace was filled with the same gas. After completely sealing the bottle using a rubber stopper, sonication was applied to the suspension for 20 min, which induces bubble coalescence [27]. To ensure equilibrium in gas molecule partitioning between the water and the headspace as well as to restore the bottle temperature back to 25 °C after being heated by sonication, the bottle was gently agitated in a 25 °C water bath overnight. Afterwards, the head space gas pressure was measured using a digital pressure gauge (PDS-B15M, Ulfatech, Seoul, Korea), which allowed the differential pressure measurement down to 0.01-mm H_2O (0.098 Pa) resolution. Applying the ideal gas law and Henry's law

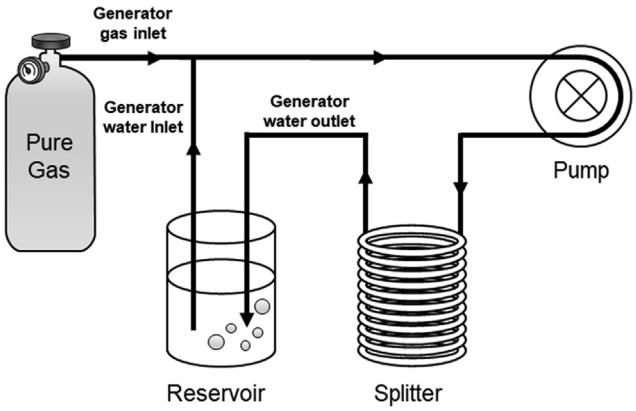

Fig. 1. Configuration of ultrafine bubble generator.

for gases in the head space and the water at the point of pressure measurement, the total gas content was determined as follows:

$$C_T = C_g + C_{aq} = (V^h/V^s)\cdot(p_g{}^f - p_g{}^i)/(R\cdot T) + p_g{}^f/H_{pc} \quad (11)$$

where $p_g{}^f$ and $p_g{}^i$ (Pa) are the final and initial gas pressures, respectively; and V^h and V^s (m^3) are the head space and suspension volume, respectively. The exact values of V^h and V^s were measured after the head space gas pressure measurement. H_{pc} values of 7.667×10^5, 1.621×10^6, and 2.903×10^6 N m mol^{-1} were used for oxygen, nitrogen, and helium, respectively [28]. The digital pressure gauge provided the pressure difference between the head space of the bottle and the laboratory atmosphere at the point of pressure measurement, whereas $p_g{}^i$ is represented by the atmospheric pressure in the laboratory during bubble suspension sampling. The signal given by the pressure gauge ranged from 545 to 740 mm H_2O (535–726 Pa), which was substantially higher than the typical 24-h variation of atmospheric pressure of <10 mm H_2O (deduced from the analysis of hourly-monitored sea-level pressure database during the year of 2017 in the monitoring station of Seoul, South Korea; http://www.weather.go.kr/weather/observation/aws_table_popup.jsp). Therefore, the pressure difference signal obtained from the pressure gauge was directly used as the difference between the final and initial gas pressure (i.e., $p_g{}^f - p_g{}^i$).

3.4. Alternative measurement of total oxygen content

For an oxygen ultrafine bubble suspension, an alternative method was employed to verify the accuracy of the head space gas pressure measurement technique. The alternative measurement method benchmarked a procedure developed by Kikuchi et al. (2009) [5], who diluted an ultrafine bubble suspension using a sufficient amount of de-oxygenated water to dissolve all bubbles into water and obtain the final dissolved oxygen (DO) concentration under the saturation level. The DO of the diluted solution can be determined either using a standard DO meter or the Winkler method, the results of which corresponded well with each other [5].

To avoid oxygen loss during dilution, the experiment in the current study was conducted using gas-tight devices. Firstly, a 0.5-mL aliquot of oxygen bubble suspension was sampled in a 3-mL gas-tight syringe. The solution for dilution was prepared by taking 49.5 mL of DI water in a 50-mL gas-tight syringe, which had been deoxygenated by purging nitrogen for at least 60 min. The DO concentration of the deoxygenated water was measured using a DO meter (ProODO, YSI Inc., USA) prior to sampling using the syringe. After connecting the two syringes using a silicon tubing, the deoxygenated water was slowly injected to the oxygen bubble suspension until the 3-mL syringe was completely filled. Then, the contents of the 3-mL syringe were injected back to the larger syringe. This procedure was repeated 10 times for complete mixing of the two solutions. The DO concentration of the diluted solution was determined using a DO meter.

3.5. Instrumental measurement of bubble diameter

The bubble diameter was directly measured using the dynamic light scattering (DLS) technique. A Zetasizer Nano system (Malvern Instruments Ltd., UK) was employed to acquire the scattered light intensity with the speckle pattern. The Stokes-Einstein equation and the Rayleigh equation were used to correlate the signals with the bubble diameter. The Rayleigh equation is written as follows:

$$I = I_0\frac{(1+cos^2\theta)}{2d^2}\left(\frac{2\pi}{\lambda}\right)^4\left[\frac{(n_2-n_1)^2-1}{(n_2-n_1)^2+2}\right]\left(\frac{D}{2}\right)^6 \quad (12)$$

where I is the intensity of light scattered by a single small particle; I_0 is the intensity of incident light; θ is the scattering angle; d is the distance to the particle; λ is the wavelength of light; and n_1 and n_2 are the refractive indices of the particle and the medium, respectively. A 4-mL aliquot of the ultrafine bubble suspension generated in a 500-mL reservoir was transferred to a quartz cuvette for the DLS analysis. Snapshots of light scattering were taken multiple times 0.5–20 min after transferring the bubble suspension into the cuvette, each of which was translated into a bubble size distribution histogram. No significant changes in the bubble size distribution curve were identified within the duration at which the snapshots were taken.

4. Results and discussion

4.1. Total gas content (C_T) and bubble volume concentration (BVC)

Interestingly, an extraordinarily high values of total gas content (C_T) are determined for the three pure-gas (i.e., oxygen, nitrogen, and helium) ultrafine bubble suspensions. The C_T values are 9.55 ± 1.79 mol m^{-3} (306 ± 57 mg L^{-1}) for pure oxygen, 4.20 ± 0.35 mol m^{-3} (117 ± 10 mg L^{-1}) for pure nitrogen, and 3.78 ± 0.09 mol m^{-3} (15.1 ± 0.4 mg L^{-1}) for pure helium ultrafine bubble suspension (average ± standard deviation; $n=3$ for each). These values are factors of 7.2, 6.7, and 10.8 higher (for pure oxygen, nitrogen, and helium bubble suspension, respectively) than the saturation value of an aqueous solution (i.e., dissolved gas concentration in equilibrium with 1 atm partial pressure of the gas) at 25 °C for the corresponding gas.

Bubble volume concentration (*BVC*) measurement indicates that only a very small volume in the ultrafine bubble suspension is occupied by the bubbles. *BVC* measured for a pure oxygen bubble suspension is 0.31 ± 0.16 mL L^{-1} suspension (mean ± standard deviation; $n=3$). Very similar results are found for other pure-gas bubble suspensions (0.31 ± 0.16 mL L^{-1} for nitrogen and 0.31 ± 0.16 mL L^{-1} for helium) (see Table 1).

4.2. Comparison of the measured and calculated values of bubble diameter

The bubble diameter determined using the dynamic light scattering (DLS) method confirms that the bubbles generated in this study are in the sub-micron scale. The bubble size distribution taken using the DLS technique for any pure-gas (i.e., oxygen, nitrogen, or helium) bubble suspension show that the bubbles are within the range from 100 to 1000 nm in diameter, with appearance of a single peak slightly skewed toward the smaller side. An example of a bubble size histogram for oxygen bubbles is shown

Table 1
Total gas content (C_T) and bubble volume concentration (*BVC*) values experimentally measured using the techniques developed in this study for three pure-gas bubble suspensions. Data are shown as average ± standard deviation (n = 3).

Pure gas	O_2	N_2	He
Total gas content, C_T	9.55 ± 1.79 mol m^{-3} (306 ± 57 mg L^{-1})	4.20 ± 0.35 mol m^{-3} (117 ± 10 mg L^{-1})	3.78 ± 0.09 mol m^{-3} (15.1 ± 0.4 mg L^{-1})
Bubble volume concentration, *BVC*	0.31 ± 0.16 mL L^{-1}	0.31 ± 0.16 mL L^{-1}	0.31 ± 0.16 mL L^{-1}

in Fig. 2 and examples for nitrogen and helium bubbles in Fig. A1. A representative diameter for each measurement is determined as the median value obtained from the bubble size distribution histogram. Multiple measurements are taken for each pure-gas bubble, enabling the statistical treatment of the representative diameters for each. Accordingly, the bubble diameters are determined as 409 ± 130 nm, 458 ± 107 nm, and 279 ± 85 nm for oxygen, nitrogen, and helium ultrafine bubbles, respectively (average ± standard deviation; n = 6, 6, and 5, respectively).

The bubble diameters calculated using Eq. (9), which are derived under the assumption that the Young-Laplace equation and Henry's law are valid, and uses C_T and *BVC* as two experimentally-measured input variables, correspond very well with the bubble diameters measured using the DLS technique. The calculated bubble diameters are 483 ± 117 nm, 518 ± 49 nm, and 304 ± 8 nm (average ± standard deviation; n = 3 for each) for oxygen, nitrogen, and helium pure-gas bubbles, respectively. For all cases, the calculated diameters and the DLS-measured diameters are statistically invariant (ANOVA, $p > 0.2$), confirming the validity of Eq. (9) for sub-micron bubble suspensions generated using three different types of pure gases.

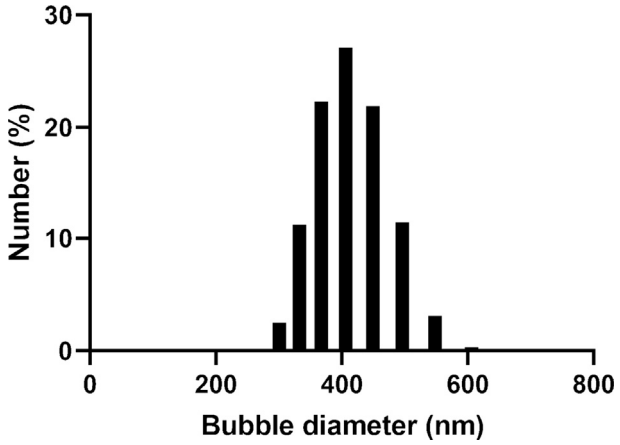

Fig. 2. An example of a bubble size histogram of oxygen ultrafine bubbles obtained by a dynamic light scattering (DLS) instrument. Such size distribution diagrams are obtained multiple times for each pure-gas bubble (6 for oxygen, 6 for nitrogen, and 5 for helium).

4.3. Ultrafine bubble suspension characteristics

As Eq. (9) is developed based on the assumption that the Young-Laplace equation (Eq. (1)) and Henry's law (Eq. (2)) holds for a sub-micron bubble suspension, the validity of Eq. (9) infers that the two relationships hold for a sub-micron bubble suspension. This statement is further validated in the next subsection. In the current subsection, several key ultrafine bubble suspension characteristics that can be calculated by taking the advantage of the validity of the Young-Laplace equation and Henry's law are presented. As shown in Eqs. (4)–(6) and (11), the two relationships between the bubbles and the aqueous solution of a bubble suspension enable calculation of the gas contents in aqueous and gaseous phases (C_{aq} and C_g, respectively), the fractions of gas molecules in aqueous and gaseous phases in a suspension (R_{aq} and R_g, respectively), inner gas pressure of a bubble (p_{in}), and bubble population (n) using the experimentally measured values of C_T and *BVC*. The values calculated for each parameter for each pure-gas bubble suspension are tabulated in Table 2.

The inner gas pressure of ultrafine bubbles (p_{in}) in aqueous suspensions is notably higher than the atmospheric pressure. The calculated p_{in} values are 7.2, 6.6, and 10.5 atm for oxygen, nitrogen, and helium bubbles, respectively. As long as Henry's law holds for gas molecule partitioning between aqueous and gaseous phases, this high inner gas pressure is associated with a highly supersaturated gas concentration in the aqueous phase. Accordingly, very high C_{aq} values, 303, 115, and 15.1 mg/L for oxygen, nitrogen, and helium bubble suspensions, respectively, are derived. Because p_{in} equals to the partial pressure of a certain pure gas, Henry's law returns a supersaturation ratio (i.e., dissolved gas concentration relative to the equilibrium value at a partial gas pressure of 1 atm) of the aqueous phase exactly the same as the numerical value of p_{in} in atm unit. In other words, the supersaturation ratios in the aqueous phase are 7.2, 6.6, and 10.5 for oxygen, nitrogen, and helium bubbles, respectively.

Most interestingly, the R_{aq} and R_g values indicate that the vast majority of gas molecules in the pure-gas bubble suspensions exist in the aqueous phase, not in bubbles. For nitrogen and helium ultrafine bubble suspensions, the R_{aq} values are estimated to be 0.9784 and 0.9656, indicating that 97.84% and 96.56% of the gas molecules in the suspensions are dissolved, respectively. For oxygen, which is more soluble in water than nitrogen or helium, an even higher R_{aq} value of 0.9906 is obtained, showing that 99.06% exist in the aqueous phase while only 0.94% is in the bubbles for the ultrafine bubble suspension.

4.4. Validation of the approach

Because of the potential of the conclusions made in the current study to substantially influence the current understanding, future research, and practical applications for ultrafine bubble suspensions, the validity of the approach employed in this study is thoroughly reviewed. This includes the measurement accuracy of the two key variables used for analyses in this study (i.e., C_T and *BVC*), impacts of the measurement errors of the two variables on the conclusions made, and the appropriateness of using the bubble diameter to confirm the validity of the Young-Laplace equation and Henry's law in an ultrafine bubble suspension.

For *BVC* measurement, there are sources of errors that may challenge the accuracy of the measured values. Although the device used in this study allows volume change measurement down to 0.01-mL resolution, external factors, such as temperature variation, may result in significant errors in the determination of the suspension volume change caused by removing bubbles. A water temperature deviation by ± 0.5 °C results in the volume change from −0.64 mL to 0.65 mL for 5000.00 mL water (or from −0.13 to 0.13 mL L^{-1} suspension) at 25.0 °C. This temperature variation corresponds to the actual variation in water temperature observed in the experiment. Therefore, the water temperature may substantially influence the accuracy of the measured *BVC* value. Water

Table 2
Characteristics of three pure-gas ultrafine bubble suspensions calculated under the assumption that the Young-Laplace equation and Henry's law are valid, and using the experimentally measured values of total gas content (C_T) and bubble volume concentration (*BVC*). Data are shown as average ± standard deviation ($n = 3$).

Pure gas	Oxygen (O_2)	Nitrogen (N_2)	Helium (He)
Bubble diameter, D	483 ± 117 nm	518 ± 49 nm	304 ± 8 nm
Gas content in aqueous phase, C_{aq}	9.46 ± 1.77 mol m^{-3} (303 ± 57 mg L^{-1})	4.11 ± 0.35 mol m^{-3} (115 ± 10 mg L^{-1})	3.65 ± 0.09 mol m^{-3} (14.6 ± 0.4 mg L^{-1})
Gas content in gaseous phase, C_g	0.09 ± 0.02 mol m^{-3} (2.90 ± 0.54 mg L^{-1})	0.08 ± 0.01 mol m^{-3} (2.33 ± 0.20 mg L^{-1})	0.13 ± 0.003 mol m^{-3} (0.53 ± 0.01 mg L^{-1})
Fraction of gas molecules in aqueous phase in a bubble suspension, R_{aq}	0.991	0.980	0.965
Fraction of gas molecules in gaseous phase in a bubble suspension, R_g	0.009	0.020	0.035
Inner gas pressure, p_{in}	$7.25 \times 10^5 \pm 1.36 \times 10^5$ Pa (7.16 ± 1.34 atm)	$6.67 \times 10^5 \pm 0.56 \times 10^5$ Pa (6.58 ± 0.55 atm)	$1.06 \times 10^6 \pm 0.03 \times 10^5$ Pa (10.46 ± 0.26 atm)
Bubble population, n	$6.38 \times 10^{15} \pm 3.53 \times 10^{15}$ counts m^{-3}	$4.43 \times 10^{15} \pm 1.37 \times 10^{15}$ counts m^{-3}	$2.12 \times 10^{16} \pm 1.75 \times 10^{15}$ counts m^{-3}

evaporation during analysis, although likely to be much less significant compared to the temperature variation because the bubble suspensions are collected in a volumetric flask with very low area to volume ratio in this study, may also slightly affect the measured volume change.

The sensitivity analysis result, however, tells that the errors in *BVC* measurement have negligible impact on the bubble diameter calculated using Eq. (9). Fig. 3 shows the calculated values of bubble diameter as a function of *BVC* and C_T obtained by inserting the *BVC* value in the range of 0.01–1.0 mL L^{-1} and the C_T value in the range of 1.5–10 times the saturation value into Eq. (9). The contours represent the isodiameter lines. The results indicate that the *BVC* variation from close to zero to 1.0 mL L^{-1} does not substantially affect the bubble diameter calculation. For example, for pure oxygen bubble suspension (measured C_T = 306 mg L^{-1}), *BVC* variation from 0.01 to 1.0 mL L^{-1} results in the calculated bubble diameter variation from −1.08% to 2.49% relative to the calculated bubble diameter using the measured *BVC* value of 0.31 mL L^{-1}. Note that the error in *BVC* measurement due to water temperature variation is estimated to be in the order of 0.1 mL L^{-1} of the exact value and the standard deviation in the actual measurement is 0.17 mL L^{-1}. Therefore, errors in *BVC* measurement should not challenge the accuracy of the calculated bubble diameter.

Despite the relatively significant contribution of C_T on the calculated bubble diameter (see Fig. 3), the errors in the C_T value determined in this study are not likely to pose a substantial impact on the calculated bubble diameter. The C_T value is determined using the head space gas pressure measurement technique as detailed in the Materials and methods Section. The relative standard deviations of the C_T measurement for the pure-gas bubble suspensions ($n = 3$ for each) are 18.7%, 8.3%, and 2.4% for oxygen, nitrogen, and helium, respectively. These values are much smaller than the relative standard deviations of the *BVC* measurement (55% for all the three pure-gas bubble suspensions), indicating that a much more precise measurement is possible for the C_T values. As discussed in the Materials and methods Section, less than 2% error is expected for the measurement of the head space pressure difference before and after the ultrafine bubble coalescence. Henry's law is applied to the bottle containing water and head space to determine the experimental C_T value from the head space pressure difference (see Eq. (11)). Because the head space pressure in the bottle is less than 2 atm, the applicability of Henry's law is not in doubt. For pure oxygen ultrafine bubble suspension, the accuracy of the C_T value determined using the head space gas pressure measurement technique is further assessed by comparing it with the result obtained from an alternative measurement technique. By diluting the oxygen ultrafine bubble suspension using a deoxygenated water and measuring the DO value of the diluted solution, the C_T value is determined to be 323 ± 16 mg L^{-1} (average ± standard deviation; $n = 3$), which corresponds very well with the C_T value determined using the head space pressure difference method (Student's *t*-test, $p = 0.32$).

Because of almost negligible contribution of *BVC* on the calculated bubble diameter for a sufficiently small value of *BVC*, the bubble diameter can be calculated using C_T as the only measured variable within this *BVC* range. Applying a *BVC* value of zero, Eq. (9) reduces to:

$$D = 4\gamma/\{H_{pc} \cdot C_T - p_{out}\} \tag{13}$$

Approximation of Eq. (9) using Eq. (13) is valid within 5% error for the following condition:

$$BVC < \{(R \cdot T)/H_{pc}\} \cdot (H_{pc} \cdot C_T - 0.05p_{out})/(0.95H_{pc} \cdot C_T + 0.05p_{out}) \tag{14}$$

For the combination of H_{pc} and C_T values for the three pure-gas ultrafine bubble suspensions in this study, $H_{pc} \cdot C_T$ is at least 6-fold greater than p_{out} (i.e., more than two orders of magnitude greater than $0.05p_{out}$). In this condition, Eq. (14) is approximated by:

$$BVC < (R \cdot T)/(0.95H_{pc}) \tag{15}$$

Eq. (15) indicates that if 5% error is acceptable and also if *BVC* values are less than 34, 16, and 9 mL L^{-1} for oxygen, nitrogen, and helium bubble suspensions, respectively, at 25 °C, measurement of *BVC* is not necessary for bubble diameter calculation purpose.

The errors associated with the determination of p_{in}, C_g, C_{aq}, R_g, R_{aq}, and n are as follows. The sensitivity analysis results for these parameters as functions of C_T and *BVC* are presented in Fig. A2. The results for C_{aq} and p_{in} are similar to that for bubble diameter; these parameters are highly sensitive to C_T whereas *BVC* measurement errors are not likely to significantly influence the accuracy of these parameters. These results are expectable from the following facts: ($p_{in} - p_{out}$) is inversely proportional to bubble diameter according to the Young-Laplace equation (Eq. (1)), p_{in} is substantially greater than p_{out} for ultrafine bubbles, and C_{aq} is proportional to p_{in} (Eq. (5)). R_g and R_{aq} are dependent only on *BVC* as can be seen from Eqs. (7) and (8). However, the errors involved in *BVC* measurements are not likely to challenge the conclusion that R_{aq} is close to unity. *BVC* measurement error of 0.1 mL L^{-1} results in less than 0.5% error in the calculated R_{aq} value. C_g and n are sensitive to both C_T and *BVC*, and errors associated with the C_T and *BVC* measurement are likely to result in significant errors in the calculated values of C_g and n.

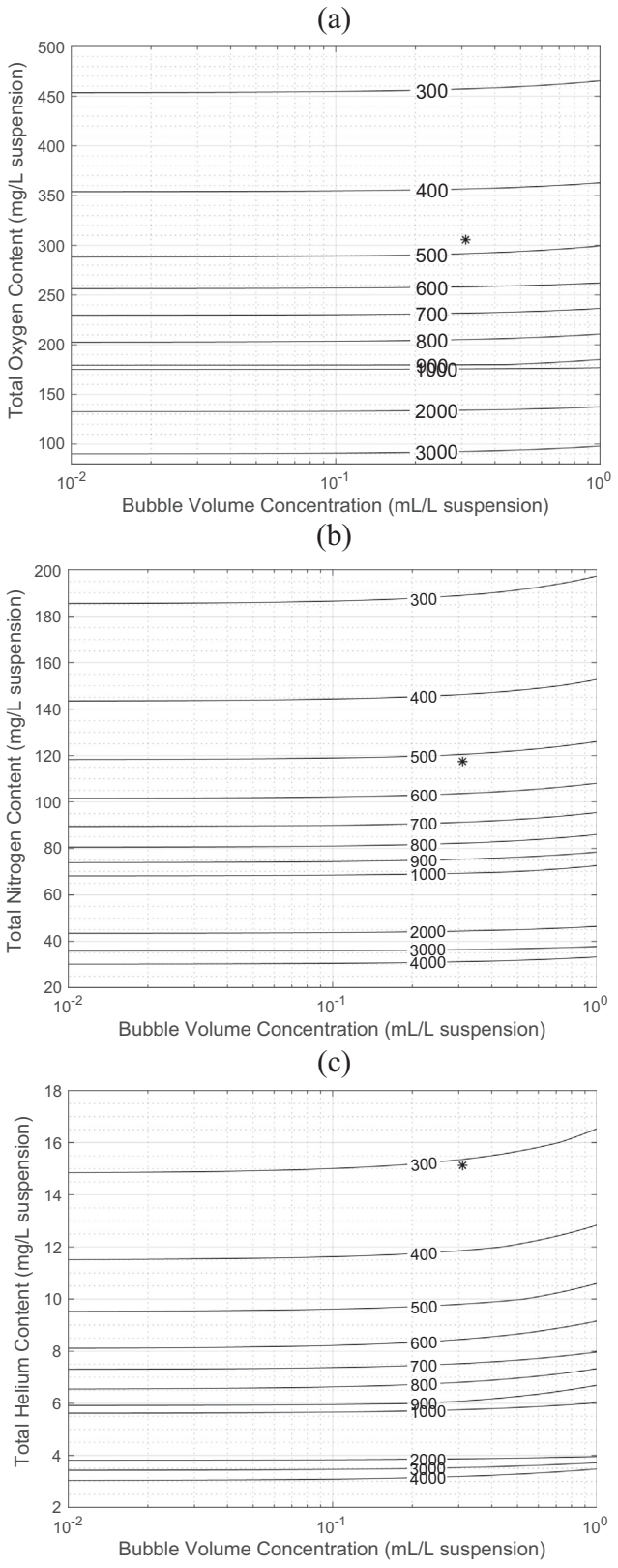

Fig. 3. Sensitivity of the calculated values of ultrafine bubble diameter to *BVC* and C_T in the case of (a) pure oxygen, (b) pure nitrogen, and (c) pure helium bubble suspensions. The contours represent the isodiameter line and the asterisk (*) represents the experimentally measured value.

The validity of using bubble diameter as a reference to examine the validity of the Young-Laplace equation and Henry's law can be confirmed by the high sensitivity of the calculated bubble diameter to the surface tension (γ) and the Henry's law constant (H_{pc}). Firstly, from Eq. (9), it is seen that the calculated bubble diameter is directly proportional to the surface tension. Eq. (13), when combined with the fact that $H_{pc}\cdot C_T$ is at least a factor of 6 greater than p_{out} in this study, implies that the calculated bubble diameter is nearly inversely proportional to the Henry's law constant. Sensitivity analysis results shown in Fig. A3 and Table A1 further confirms this relationship. Therefore, the calculated bubble diameter can be approximated to be proportional to γ/H_{pc}. Assuming that Henry's law holds exactly for sub-micron-sized bubbles (i.e., ${H_{pc}}^B = {H_{pc}}^A$; where ${H_{pc}}^B$ and ${H_{pc}}^A$ are the Henry's law constants applicable for a bubble suspension and at ambient conditions, respectively), the calculated and DLS-measured bubble diameter being statistically invariant indicates that γ^B and γ^A are also statistically invariant. A similar conclusion could be made for the correspondence of ${H_{pc}}^B$ with ${H_{pc}}^A$ assuming $\gamma^B = \gamma^A$. Mathematically, it is possible that $\gamma^B/\gamma^A \sim {H_{pc}}^B/{H_{pc}}^A$ such that $\gamma/\mathrm{H_{pc}}$ remains to be nearly constant whereas H_{pc} and γ values in sub-micron bubble suspensions significantly deviate from their values at ambient conditions. However, it is hardly imaginable that this condition is accidently met for all the three pure-gas bubble suspensions examined in this study, which exhibit substantially different total gas contents with one another. It should also be pointed out that according to a previous study that derived an empirical relationship between gas pressure and water surface tension by experimental measurement of the surface tension under dense gas atmospheres [29], the p_{in} values for the three pure-gas ultrafine bubbles calculated in the current study are estimated to result in less than 1% reduction in water surface tension.

A noteworthy underlying assumption for the discussion given above is that the DLS technique provides an accurate measurement of bubble diameter. DLS technique is one of the most frequently used method to determine bubble diameter for sub-micron-sized bubbles [30]. The technique is used to estimate sizes of sub-micron- or nano-sized particles by measuring light scattering which is a function of the size and reflective index of an object. The Rayleigh's equation given in Eq. (12) indicates that the accuracy of the DLS measurement depends on the difference in the refractive index between the particle and the medium. Because the refractive index of a gas-phase particle (~1.00) and that of water (~1.33) are substantially different, the size of ultrafine bubbles can be accurately measured by the DLS technique.

4.5. Implications

The improved knowledge on the characteristics and behavior of bulk ultrafine bubbles enabled by the current study presents important implications that should be considered for relevant research and applications. In addition, the study implies that follow-up works are necessary to further explore the behavior of bulk ultrafine bubbles generated in various conditions and present in different environments.

The current study provides a simple and easy-to-follow technique to estimate the diameter of sub-micron-sized bubbles. In the scientific field, challenges in bubble diameter estimation, including the limited availability of specialized instruments and concerns involved in the transport of a bubble suspension from the point of generation to the instrument, have been one of the major bottleneck for initiating an ultrafine bubble research. These challenges also limit the current ability to evaluate the performance of bubble-generating devices available in the market. As demonstrated above, in most cases, diameter of bubbles generated using a pure gas can be calculated using the total gas content as the only measured parameter. The total gas content measurement does not require any specialized devices or instruments, allowing

the measurement viable in any laboratory settings. By the measurement technique, a representative bubble diameter for a bubble suspension is obtained, which is directly related to other bubble suspension characteristics such as inner pressure of the bubble and dissolved gas concentration in the suspension. Therefore, the representative bubble diameter determined by the total gas content measurement is expected to more adequately represent the bubble suspension characteristics than the value (or the range of values) determined by specialized instruments.

To further extend the applicability of the proposed technique, it should be investigated if the technique is available for determining the diameter of bubbles generated using a mixture of gases (e.g., ambient air). An extensive set of research may be needed because much greater complexity is expected for mixed-gas ultrafine bubbles. The gas composition in the bubbles may not be the same as the gas composition of the air used for the bubble generation, and accordingly, improved understanding on the bubble suspension characteristics and gas molecule behavior is required for the application of the proposed technique.

The validity of the Young-Laplace equation and Henry's law for sub-micron-sized bubbles provides significant implications for bubble behavior in a suspension. The two theories imply that the most thermodynamically favorable size of a pure-gas bubble is determined by the aqueous concentration of the gas in the suspension. The small R_g value estimated in this study suggests that the gases in aqueous phase serves as almost an infinite reservoir for bubble formation. Therefore, in the absence of significant loss of gas molecules from a bubble suspension and under negligible interactions between the gas molecules and the inner surface of the container, bubbles once generated in different sizes are likely to evolve into the size that satisfies the Young-Laplace equation and Henry's law. Once the bubbles are evolved into the size offering thermodynamic stability, the bubble suspension may stay stable as far as the bubble movement is dictated by Brownian motion (i.e., the bubble rising velocity is negligible). In addition, an increase in the aqueous concentration is expected to induce bubble shrinkage. Likewise, a decrease in the aqueous concentration is expected to result in bubble size growth, and if the decrease continues, the bubble will be grown to finally exhibit a rising velocity sufficient for bubble rise and disappearance. The latter phenomenon is likely to occur when an ultrafine bubble suspension is placed in an open vessel, where a driving force for gas molecule mass transfer should exist such that the supersaturated gas in the aqueous phase will be released to the atmosphere. We believe that the gas molecule mass transfer from the suspension to the atmosphere is one of the key mechanisms that determine the stability of ultrafine bubbles.

The current study demonstrates that a highly supersaturated gas solution could be obtained using an ultrafine bubble generator. This observation implies that, by generating ultrafine bubble suspensions using reactive gases such as ozone or hydrogen, a solution with very high activities for such gases could be achieved, allowing significantly improved reaction rates and providing redox potentials sufficient to break down highly recalcitrant compounds. Currently, there is rapid growth of scientific research to improve the reactivity of gas molecules by employing ultrafine bubble suspensions [31,32]. It is recommended for these studies to investigate the relationship between the dissolved gas concentration and the chemical reactivity, and to explore ways to better utilize the high dissolved gas concentration achievable via ultrafine bubble generation. Another line of current scientific research employing ultrafine bubble suspensions is to enhance the transport of gas molecules through environmental media such as aquifer materials [9,33]. The current study results indicate that the majority of the gas molecules in an ultrafine bubble suspension is essentially in dissolved phase. Therefore, the role of the aqueous medium as a carrier of gas molecules should be considered as significant. Of course, the characteristics of a bubble suspension is likely to change substantially when the suspension is injected in porous media, and this dynamic behavior of gas molecules should be fully investigated in the future.

Due to their significant implications as stated above, studies are needed to further verify the conclusions of the current study. We used bubble size as a key parameter to validate our hypothesis that the Young-Laplace equation and Henry's law holds for sub-micron-sized bubbles because of the current availability to measure the bubble diameter using instrumental techniques. Development of a measurement technique for inner pressure of bubbles will help further validate the hypothesis of the current study. This study is conducted at a fixed temperature of 25 °C, and thus it is necessary to examine the validity of the Young-Laplace equation and Henry's law at different temperatures at which the surface tension of water and Henry's law constants of gases are different from those applied in the current study.

5. Conclusion

Despite the large volume of literature reporting the high stability of ultrafine bubbles in aqueous suspensions [2–5], the thermodynamic equilibrium at the gas-water interface in the suspension, which is essential to describe the observed stability, is yet to be defined [18,20]. Specifically, it has been questionable whether the two classical theories (i.e., the Young-Laplace equation and Henry's law) that have been used to describe the thermodynamic equilibrium at conventionally studied gas-water interfaces are applicable to ultrafine bubbles [17,21]. By studying aqueous suspensions of sub-micron-sized bubbles generated using three pure gases, we clearly demonstrate that the Young-Laplace equation and Henry's law are applicable to the gas molecule behavior in the suspensions. With a hypothesis that the two theories are valid, we derive an equation that enables calculating bubble diameter using gross characteristics of the bubble suspension (i.e., C_T and BVC). The calculated bubble diameter corresponds very well with the bubble diameter directly measured by a dynamic light scattering technique. By sensitivity analyses, we show that the correspondence of the calculated and directly measured bubble diameters can reasonably be used to conclude that the two theories are valid to sub-micron-sized bubbles. Because the Young-Laplace equation and Henry's law define the relationships among key variables that characterize a bubble suspension, when one or two of the key variables are experimentally determined for a sub-micron-sized bubble suspension, the rest of the variables may be determined by utilizing the relationships. We show in this paper that p_{in}, C_g, C_{aq}, R_g, R_{aq}, and n for a bubble suspension can be derived from the experimentally determined values of C_T and BVC. The values of the key variables determined for three pure-gas bubble suspensions in this study suggest that most of the gas molecules in the bubble suspensions exist in the aqueous phase, which present significant implications for the application of the bubble suspensions for chemical reactions, gas molecule transfer and transport, among others. Further studies are recommended to examine the validity of the Young-Laplace equation and Henry's law in more complex systems than is studied in the current study, including mixed gas bubble suspensions and bubble suspensions present in porous media.

CRediT authorship contribution statement

Euna Kim: Methodology, Formal analysis, Investigation, Writing - original draft, Visualization. **Jong Kwon Choe:** Supervision. **Byung Hyo Kim:** Validation, Writing - original draft. **Joodeok Kim:** Data curation. **Jungwon Park:** Resources, Supervision. **Yongju Choi:** Conceptualization, Supervision, Writing - review & editing, Project administration.

Declaration of Competing Interest

The authors declare that they have no known competing financial interests or personal relationships that could have appeared to influence the work reported in this paper.

Acknowledgement

This work was supported by the Korea Institute of Energy Technology Evaluation and Planning (KETEP) and the Ministry of Trade, Industry & Energy (MOTIE) of the Republic of Korea (No. 20181510300800). The authors would like to thank Dr. Tschung-il Kim at Seoul National University and Dr. Tatek Temesgen at Adama Science and Technology University (formerly at Seoul National University) for kind advices on our experimental setup. The authors also would like to thank the Institute of Engineering Research at Seoul National University for technical assistance.

Appendix A. Supplementary material

Supplementary data to this article can be found online at https://doi.org/10.1016/j.jcis.2020.02.101.

References

[1] T. Fujita, Fine bubble technology, Int. Organ. Stand. ISO/TC (2018). http://pasc2018.jsa.or.jp.
[2] F.Y. Ushikubo, T. Furukawa, R. Nakagawa, M. Enari, Y. Makino, Y. Kawagoe, T. Shiina, S. Oshita, Evidence of the existence and the stability of nano-bubbles in water, Colloids Surf. A Physicochem. Eng. Asp. 361 (2010) 31–37, https://doi.org/10.1016/j.colsurfa.2010.03.005.
[3] T. Uchida, S. Oshita, M. Ohmori, T. Tsuno, K. Soejima, S. Shinozaki, Y. Take, K. Mitsuda, Transmission electron microscopic observations of nanobubbles and their capture of impurities in wastewater, Nanoscale Res. Lett. 6 (2011) 1–9, https://doi.org/10.1186/1556-276X-6-295.
[4] K. Yasui, T. Tuziuti, W. Kanematsu, Mysteries of bulk nanobubbles (ultrafine bubbles); stability and radical formation, Ultrason. Sonochem. 48 (2018) 259–266, https://doi.org/10.1016/j.ultsonch.2018.05.038.
[5] K. Kikuchi, A. Ioka, T. Oku, Y. Tanaka, Y. Saihara, Z. Ogumi, Concentration determination of oxygen nanobubbles in electrolyzed water, J. Colloid Interface Sci. 329 (2009) 306–309, https://doi.org/10.1016/j.jcis.2008.10.009.
[6] V.S.J. Craig, Very small bubbles at surfaces - the nanobubble puzzle, Soft Matter 7 (2011) 40–48, https://doi.org/10.1039/c0sm00558d.
[7] M. Matsumoto, K. Tanaka, Nano bubble-Size dependence of surface tension and inside pressure, Fluid Dyn. Res. 40 (2008) 546–553, https://doi.org/10.1016/j.fluiddyn.2007.12.006.
[8] L. Hu, Z. Xia, Application of ozone micro-nano-bubbles to groundwater remediation, J. Hazard. Mater. 342 (2018) 446–453, https://doi.org/10.1016/j.jhazmat.2017.08.030.
[9] H. Li, L. Hu, D. Song, A. Al-Tabbaa, Subsurface transport behavior of micro-nano bubbles and potential applications for groundwater remediation, Int. J. Environ. Res. Public Health. 11 (2013) 473–486, https://doi.org/10.3390/ijerph110100473.
[10] Z. Wu, X. Zhang, X. Zhang, J. Sun, Y. Dong, J. Hu, In situ AFM observation of BSA adsorption on HOPG with nanobubble, Chinese Sci. Bull. 52 (2007) 1913–1919, https://doi.org/10.1007/s11434-007-0288-8.
[11] A. Gurung, O. Dahl, K. Jansson, The fundamental phenomena of nanobubbles and their behavior in wastewater treatment technologies, Geosyst. Eng. 19 (2016) 133–142, https://doi.org/10.1080/12269328.2016.1153987.
[12] K. Ebina, K. Shi, M. Hirao, J. Hashimoto, Y. Kawato, S. Kaneshiro, T. Morimoto, K. Koizumi, H. Yoshikawa, Oxygen and air nanobubble water solution promote the growth of plants, fishes, and mice, PLoS One. 8 (2013) 2–8, https://doi.org/10.1371/journal.pone.0065339.
[13] S. Liu, Y. Kawagoe, Y. Makino, S. Oshita, Effects of nanobubbles on the physicochemical properties of water: the basis for peculiar properties of water containing nanobubbles, Chem. Eng. Sci. 93 (2013) 250–256, https://doi.org/10.1016/j.ces.2013.02.004.
[14] R. Cavalli, A. Bisazza, P. Giustetto, A. Civra, D. Lembo, G. Trotta, C. Guiot, M. Trotta, Preparation and characterization of dextran nanobubbles for oxygen delivery, Int. J. Pharm. 381 (2009) 160–165, https://doi.org/10.1016/j.ijpharm.2009.07.010.
[15] C. Magnetto, M. Prato, A. Khadjavi, G. Giribaldi, I. Fenoglio, J. Jose, G.R. Gulino, F. Cavallo, E. Quaglino, E. Benintende, G. Varetto, A. Troia, R. Cavalli, C. Guiot, Ultrasound-activated decafluoropentane-cored and chitosan-shelled nanodroplets for oxygen delivery to hypoxic cutaneous tissues, RSC Adv. 4 (2014) 38433–38441, https://doi.org/10.1039/c4ra03524k.
[16] J.R. Eisenbrey, L. Albala, M.R. Kramer, N. Daroshefski, D. Brown, J.-B. Liu, M. Stanczak, P. O'Kane, F. Forsberg, M.A. Wheatley, Development of an ultrasound sensitive oxygen carrier for oxygen delivery to hypoxic tissue, Int. J. Pharm. 478 (2015) 361–367, https://doi.org/10.1016/j.ijpharm.2014.11.023.
[17] M. Alheshibri, J. Qian, M. Jehannin, V.S.J. Craig, A history of nanobubbles, Langmuir 32 (2016) 11086–11100, https://doi.org/10.1021/acs.langmuir.6b02489.
[18] N. Nirmalkar, A.W. Pacek, M. Barigou, On the existence and stability of bulk nanobubbles, Langmuir 34 (2018) 10964–10973, https://doi.org/10.1021/acs.langmuir.8b01163.
[19] A. Azevedo, R. Etchepare, S. Calgaroto, J. Rubio, Aqueous dispersions of nanobubbles: generation, properties and features, Miner. Eng. 94 (2016) 29–37, https://doi.org/10.1016/j.mineng.2016.05.001.
[20] J.W.G. Tyrrell, P. Attard, Atomic force microscope images of nanobubbles on a hydrophobic surface and corresponding force-separation data, Langmuir 18 (2002) 160–167, https://doi.org/10.1021/la0111957.
[21] P. Attard, The stability of nanobubbles, Eur. Phys. J. Spec. Top. (2013) 1–22, https://doi.org/10.1140/epjst/e2013-01817-0.
[22] P.S. Epstein, M.S. Plesset, On the stability of gas bubbles in liquid-gas solutions, J. Chem. Phys. 18 (1950) 1505–1509, https://doi.org/10.1063/1.1747520.
[23] P.K. Jain, X. Huang, I.H. El-sayed, M.A. El-sayed, Noble metals on the nanoscale: optical and photothermal properties and some applications, Acc. Chem. Res. 41 (2008) 7–9, https://doi.org/10.1021/ar7002804.
[24] P.M. Ajayan, Nanotubes from carbon, Chem. Rev. 99 (2002) 1787–1800, https://doi.org/10.1021/cr970102g.
[25] C.P. Bean, J.D. Livingston, Superparamagnetism, J. Appl. Phys. 30 (1959) S120–S129, https://doi.org/10.1063/1.2185850.
[26] H.J. Hoge, C.H. Meyers, R.E. McCoskey, Charts of compressibility factors and charts showing quantities delivered by commercial cylinders hydrogen, nitrogen, and oxygen, Natl. Bur. Stand. (1948).
[27] K. Yasuda, H. Matsushima, Y. Asakura, Generation and reduction of bulk nanobubbles by ultrasonic irradiation, Chem. Eng. Sci. 195 (2019) 455–461, https://doi.org/10.1016/j.ces.2018.09.044.
[28] R. Sander, Compilation of Henry's law constants (version 4.0) for water as solvent, Atmos. Chem. Phys. 15 (2015) 4399–4981, https://doi.org/10.5194/acp-15-4399-2015.
[29] R. Massoudi, A.D. King, Effect of pressure on the surface tension of water. Adsorption of low molecular weight gases on water at 25°, J. Phys. Chem. 78 (1974) 2262–2266, https://doi.org/10.1021/j100615a017.
[30] L. Yang, Y. Wang, X. Li, D. Pan, L. Li, J. Peng, L. Hou, Z. Chen, Rapid determination of a fluorinated gas in a lipid microbubble contrast agent by ultrasound-mediated microbubble destruction and GC-MS, Anal. Methods 8 (2016) 3353–3358, https://doi.org/10.1039/c5ay01912e.
[31] D. Wang, X. Yang, C. Tian, Z. Lei, N. Kobayashi, M. Kobayashi, Y. Adachi, K. Shimizu, Z. Zhang, Characteristics of ultra-fine bubble water and its trials on enhanced methane production from waste activated sludge, Bioresour. Technol. 273 (2019) 63–69, https://doi.org/10.1016/j.biortech.2018.10.077.
[32] X. Yang, J. Nie, D. Wang, Z. Zhao, M. Kobayashi, Y. Adachi, K. Shimizu, Z. Lei, Z. Zhang, Enhanced hydrolysis of waste activated sludge for methane production via anaerobic digestion under N2-nanobubble water addition, Sci. Total Environ. 693 (2019), https://doi.org/10.1016/j.scitotenv.2019.07.330 133524.
[33] F. Malard, F. Hervant, Oxygen supply and the adaptations of animals in groundwater, Freshw. Biol. 41 (2003) 1–30, https://doi.org/10.1046/j.1365-2427.1999.00379.x.